

Fig. 2. Proposed system architecture.

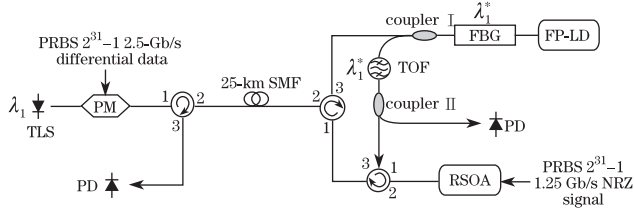


Fig. 3. Experimental setup.

a DPSK signal detector and wavelength converter. This way, the recovered intensity data can be transferred to another cavity mode for upstream transmission, thereby mitigating RB noise. In an optical line terminal (OLT), downstream data are modulated on continuous wave (CW) light λ_i by a phase modulator. The multiplexed wavelengths are transmitted to a remote node (RN) after transmission over 25-km optical fiber. Optical carriers are then demultiplexed and routed to different ONUs. In each ONU, a FBG-based self-seeding FP-LD is driven by an externally injected downstream wavelength. Because a sudden phase shift in DPSK signals can cause frequency deviation in optical carriers, the unstable injection locking state in the FP-LD caused by downstream DPSK signals results in intensity fluctuations. Furthermore, phase information is converted into intensity data from cavity mode λ_i to λ_i^* through the destroyed self-seeding condition at wavelength λ_i^* . Converted wavelength λ_i^* is filtered by a TOF and subsequently split by a 50:50 optical coupler. One split beam is detected by a photo detector (PD) to recover downstream data. The other beam is sent to the RSOA as seeding light to remodulate upstream non-return-to-zero (NRZ) data. To satisfy the requirements for wavelength independence, both the FBG and TOF have tunable functions that can flexibly change the central wavelength. These functions ensure the colorless characteristic of ONUs.

We first investigate the performance of the proposed DPSK signal demodulation and wavelength conversion scheme in WDM-PONs with injection-locked FP-LDs. In the experimental setup (Fig. 3), the input wavelength λ_1 (1543.68 nm) is generated by a tunable laser source with a power of 6 dBm, modulated with pseudo-random binary sequence (PRBS) with a length of $2^{31}-1$. After propagating through 25-km SMF and two circulators, the signal is transmitted to a self-seeding FP-LD. This FP-LD is in an injection locking state at wavelength λ_1^* (1542.27 nm), which corresponds to one longitude mode with a peak power of 3 dBm and side mode suppression ratio of nearly 50 dB (Fig. 4(a)). The bias current and operating temperature of the FP-LD can be controlled to a wide wavelength tuning range up to 30 nm (from 1530 to 1560 nm).

The 30-GHz frequency deviation range induced by the 16.5-ps rise time of differential intensity data results in an

unstable injection locking state; that is, frequency deviation that corresponds to every phase shift in wavelength λ_1 occurs. If deviation is larger than locking range, the FP-LD becomes unlocked. Given that the phase remains constant, no frequency deviation is observed and the FP-LD is in a stable locking state. The locking and unlocking states in longitude mode λ_1 can be converted into intensity data. On the basis of this principle, mode λ_1^* is suppressed to a certain level (suppression ratio, ~ 17 dB) and the peak power of longitude mode λ_1 is 5.8 dBm when DPSK signal λ_1 is injected at an adjacent wavelength near dominant mode λ_1^* (Fig. 4(b)). Unlike the original longitude mode, external injection locking introduces a 0.1-nm red shift, consequently destroying the wavelength alignment on FBG. When longitude mode λ_1 is unlocked, mode λ_1^* returns to a locking state. In this manner, every phase shift is converted into intensity data from mode λ_1 to mode λ_1^* .

We then investigate the transmission properties of the proposed WDM-PON system. A specific analysis of downstream and upstream BER performance is carried out to verify the application of the DPSK signal demodulation and wavelength conversion scheme. The total transmission loss is 13 dB, including that generated by 25-km SMF transmission. A pre-amplified PD is used as a receiver in the ONU. Unlike the MZDI, the FP-LD measures a power penalty of 1.6 dB at a BER of 10^{-9} (Fig. 5(a)). This result is due to the decreased extinction ratio (about 2.1 dB) and additional noise from the loop back structure in the ONU. As shown in Fig. 5(b), when the same wavelength is used for upstream transmission, the eye diagram is severely distorted and the BER cannot reach the lowest requirement of 10^{-9} . Through wavelength conversion by the self-seeding FP-LD, however, downstream wavelength λ_1 and upstream wavelength λ_1^*

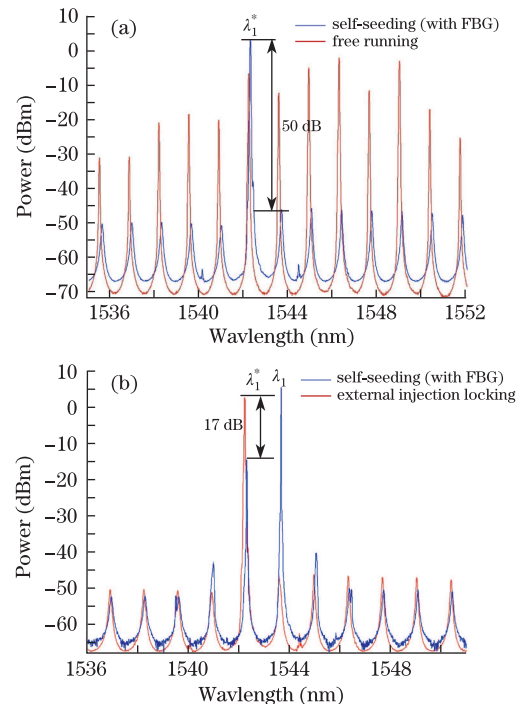


Fig. 4. Optical spectra. (a) Self-seeding at mode λ_1^* with a free running state of FP-LD; (b) external injection locking at mode λ_1 with self-seeding state.

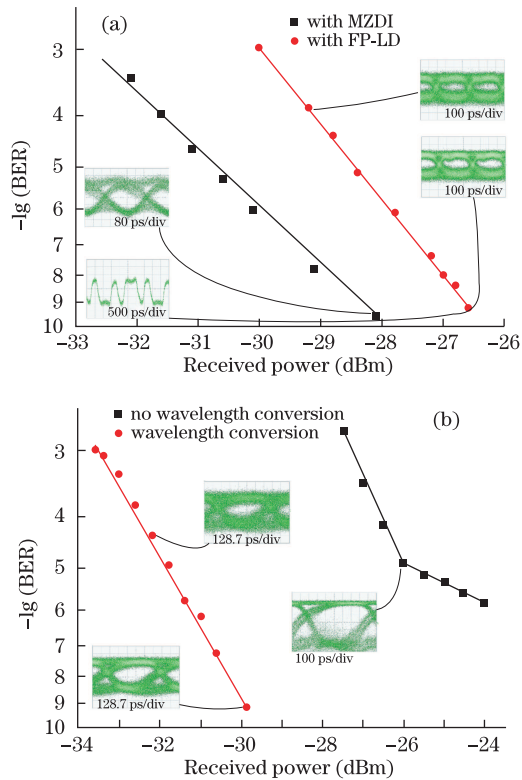


Fig. 5. BER performance, eye diagrams, and waveform. (a) Downstream; (b) upstream

are clearly distinguished, thereby effectively eliminating RB noise. Furthermore, the converted signals have a low extinction ratio. When the RSOA is operated in the gain saturation region, it can effectively erase all residual downstream data and remodulate upstream data. Thus, the eye diagram is clearly open and receiver sensitivity is about -30 dBm. When limited by the performance of a low-cost FP-LD, the highest speed for simultaneous DPSK signal demodulation and wavelength conversion is only 2.5 Gb/s. A speed of 10 Gb/s is realized by optimizing the physical parameters of the self-seeding FP-LD.

In conclusion, we propose a DPSK signal demodulation and wavelength conversion scheme based on a self-seeding FP-LD in a WDM-PON system. RB noise is effectively mitigated through wavelength conversion

and differentiation between bidirectional wavelengths. For downstream signals, a power penalty of about 1.6 dB is experimentally measured at a BER of 10^{-9} . The sensitivity of upstream transmission can reach -30 dBm without RB noise. The total working wavelengths can be increased by adjusting the bias current and operation temperature of the FP-LD. Such adjustments consequently upgrade transmission capacity.

This work was supported by the National “973” Project of China (Nos. 2010CB328205, 2010CB328204, and 2012CB315602), the National Natural Science Foundation of China (Nos. 60972032, 61090393, 61132004, and 60825103), and the National “863” Project of China.

References

1. K. Iwatsuki and J. I. Kani, *J. Opt. Commun. Netw.* **1**, C17 (2009).
2. A. Banerjee, Y. Park, F. Clarke, H. Song, S. Yang, G. Kramer, K. Kim, and B. Mukherjee, *J. Opt. Netw.* **4**, 737 (2005).
3. N. Q. Thai, P. Besnard, L. Bramerie, A. Shen, C. Kazmierski, P. Chanlou, D. Guang-Hua, and J. C. Simon, *IEEE Photon. Technol. Lett.* **22**, 733 (2010).
4. E. Wong, L. K. Lun, and T. B. Anderson, *J. Lightwave Technol.* **25**, 67 (2007).
5. X. Jing and C. Lian-Kuan, *IEEE Photon. Technol. Lett.* **22**, 456 (2010).
6. R. Murano, W. F. Sharfin, and M. J. Cahill, in *Proceedings of OFC/NFOEC 2008 PDP32* (2008).
7. “PC Controlled tunable FBG,” retrieved <http://www.aos-fiber.com/eng/FBG/FBGen.html>.
8. G. Bosco and P. Poggiolini, *J. Lightwave Technol.* **23**, 842 (2005).
9. K. Coussore, I. Kim, Y. Han, C. Kim, G. Li, and S. Radic, *Opt. Express* **13**, 3945 (2005).
10. G. Bosco, A. Coster, and V. Curri, in *Proceedings of ECOC 2006 1* (2006).
11. X. Jing, C. Lian-Kuan, and C. Chun-Kit, *IEEE Photon. Technol. Lett.* **22**, 1343 (2010).
12. C. W. Chow and C. H. Yeh, *Opt. Express* **19**, 4970 (2011).
13. G. Talli, C. W. Chow, E. K. MacHale, and P. D. Townsend, *J. Opt. Netw.* **6**, 765 (2007).